Surface Science 210 (1989) L177–L184
North-Holland, Amsterdam

SURFACE SCIENCE LETTERS

DYNAMICS OF TIP–SUBSTRATE INTERACTIONS IN ATOMIC FORCE MICROSCOPY *

Uzi LANDMAN, W.D. LUEDTKE and A. NITZAN
School of Physics, Georgia Institute of Technology, Atlanta, GA 30332, USA

Received 22 November 1988; accepted for publication 5 December 1988

Dynamical interactions between a scanning tip and a silicon substrate are investigated using molecular dynamics simulations of both the constant-height and constant-force scan modes. Localized temporary and permanent modifications of the substrate occur, depending on tip–substrate separation and scan geometry. Implications for resolving structural and force characteristics in scanning tip spectroscopies, employing atomically sharp as well as large ordered of disordered tips are discussed.

The developments of scanning tunneling microscopy [1] (STM), the related atomic force microscopy (AFM) [2], and the surface force apparatus (SFA) [3,4] revolutionized our perspectives and abilities to probe the morphological and electronic structure and the nature of interatomic forces in materials, as well as opened new avenues [5] for microscopic investigations and manipulations of technological systems and phenomena such as tribology [4,6], lithography and in biochemical applications. In both STM and AFM a tip is brought close to the surface and either the tunneling current (STM) or deflection of the cantilever holding the tip (AFM) are monitored as the surface is scanned. Of particular interest are questions related to the nature of the tip–substrate interactions and the dynamical response of the substrate (and tip) which may result in temporary or permanent modifications of the local properties [7,8] and be reflected in the recorded data.

In this paper we investigate the dynamics of the tip–substrate interactions via molecular dynamics simulations employing a realistic interatomic interaction potential for silicon (the Stillinger–Weber (SW) potential [9]) which has been used recently in a number of investigations [10–14] of bulk, surface and interface properties of this material. Since both the substrate and tip consist of the same material, these simulations correspond to the case of a reactive tip–substrate system [11–14]. Our simulations [12–14], in both the constant-

* Work supported by US DOE under grant No. FG05-86ER45234, and by the DARPA-Hughes Tribology Program.

tip-height and constant-force scan modes, reveal that the local structure of the surface can be stressed and modified as a consequence of the tip–substrate dynamical interaction, even at tip–substrate separations which correspond to weak interaction. For large separations these perturbations anneal upon advancement of the tip while permanent damage can occur for smaller separations. For the material that we simulated (Si), we do not find long-range elastic deformations, which may occur in other circumstances [7] depending upon the elastic properties of the material and the nature of interactions. The characteristics of the data depend upon the geometry of the scan, the degree of perfection of the substrate and the temperature. We identify various dynamical events including stick–slip phenomena, which could be experimentally resolved, using current estimates [1,2,5], and which would influence the analysis of data, as well as pointing to ways in which the tip could be used for atomic scale manipulations of the material.

In our simulations the system consists of 4 layers of dynamic Si particles with 49 (or 100) atoms per layer, exposing the (111) surface, and interacting with 2 layers of a static Si substrate of the same structure (calculations with systems of 6 dynamic layers and a larger number of particles/layer yield very similar results). The 2D calculational cell, defined by the $(1\bar{1}0)$ and $(10\bar{1})$ vectors, is periodically repeated parallel to the (111) plane. Two types of tips were employed in our simulations. First, we have used a sharp tip [1,2,5] simulated by 4 Si atoms in an initial tetrahedral configuration, "mounted" on and interacting with 2 layers of silicon atoms which serve as a holder. In addition we have employed larger tips consisting of 102 atoms, which were either ordered (exposing a 16 atoms (111) planar facet) or disordered. The equations of motion, governed by the SW potential [9], which contains 2- and 3-body interactions (V_2 and V_3 respectively), are integrated using a 5th order predictor–corrector algorithm with a time step $\Delta t = 1.15 \times 10^{-3}$ ps (or 0.015 tu where tu $= 7.6634 \times 10^{-14}$ s). Throughout we use $\epsilon = 50$ kcal/mol as the unit of energy, $\sigma = 2.0951$ Å as the unit of length, and $\epsilon/\sigma = 1.65728 \times 10^{-9}$ N as the unit of force. The reduced units of length X^*, Y^* and Z^*, along the $(1\bar{1}0)$, $(10\bar{1})$ and (111) directions are 12.82σ, 12.82σ, and 5.8333σ, respectively. The kinetic temperature is controlled via scaling of particle velocities in the bottom layer of the dynamic substrate.

Both constant-tip-height and constant-force scan modes were simulated. In the first mode following equilibration at room temperature, with the tip outside the range of interaction, the tip is lowered slowly (5.4×10^{-4} $\sigma/\Delta t$) to a prescribed height. Studies at 3 initial tip heights, h_i ($i = 1, 3$), corresponding to distances of 2.91, 2.345 and 1.227 Å between the lowest tip atom and the uppermost layer of the substrate, were performed. h_1, h_2 and h_3 correspond to the attractive, equilibrium, and repulsive regions of the interparticle potential, respectively. To faithfully simulate the laboratory process, which is much slower than can be achieved in computer simulations, and record data for

structurally relaxed tip–substrate configurations we have adopted the following scan and data accumulation procedure: (a) The system is first equilibrated for 200 Δt with the tip at the desired height. (b) Lateral scans (along X^* (110)) consist of: (i) equilibration for 150 Δt followed by 150 Δt of data collection and averaging, (ii) motion of the tip assembly for 50 Δt to a new scan point (8 scan points per 2D unit cell length, covering in each lateral scan 3 unit cells), after which step (i) is repeated. In exploratory studies we found that the results of the simulations are not modified in any substantial way by increasing the equilibration periods. Results for 2 lateral scans at each height are described, denoted by $h_i(1)$ for the scan on top of an atomic row, and by $h_i(2)$ for the scan mid-distance between rows.

In the constant-force simulations in addition to the particle equations of motions the center of mass of the tip-holder assembly, Z, is required to obey $M\ddot{Z} = (\boldsymbol{F}(t) - \boldsymbol{F}_{\text{ext}}) \cdot \hat{Z} - \gamma \dot{Z}$ where $\boldsymbol{F}$ is the total force exerted by the tip atoms on the static holder at time t, which corresponds to the force acting on the tip atoms due to their interaction with the substrate, $\boldsymbol{F}_{\text{ext}}$ is the desired (prescribed) force for a given scan, γ is a damping factor and M is the mass of the holder. In these simulations the system is brought to equilibrium for a

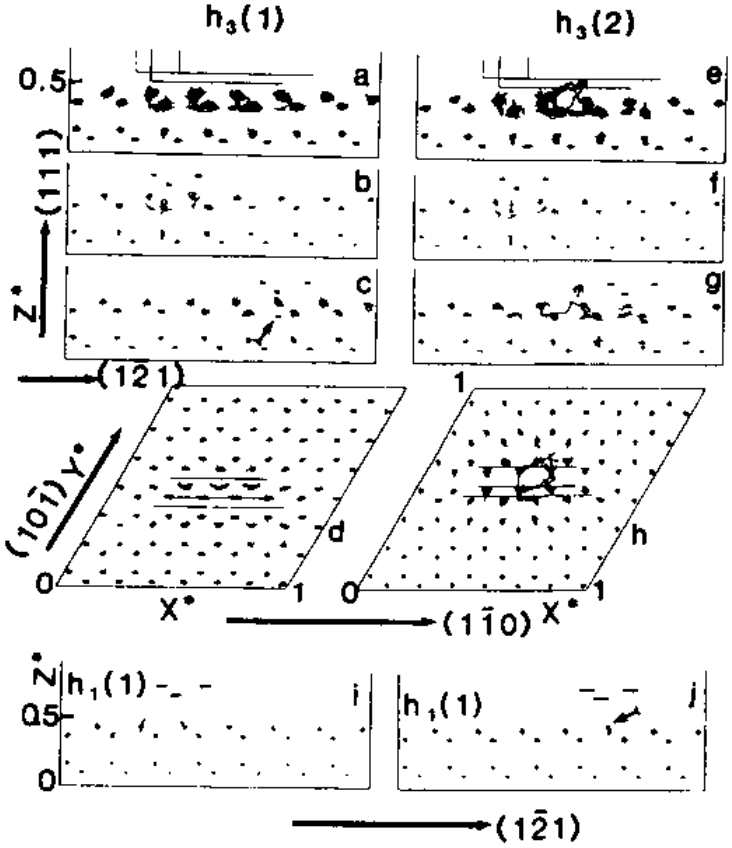

Fig. 1. (a–d) Particle trajectories for the low-tip, $h_3(1)$, scan: (a, d) complete scan; (b, c) at beginning and towards the end of the scan, respectively. In (a–c) view along the $(10\bar{1})$ direction, in (d) view along (111). (e–h) same as (a–d) for between-the-rows, $h_3(2)$, scan; note the damage caused in the substrate. (i, j) trajectories at the beginning and towards the end of the high-tip, $h_1(1)$ scan. Arrows in (c) and (j) point to induced defects. The tip atoms are located on the horizontal lines above the substrate, scanning from left to right.

prescribed value of F_{ext}, and the scan proceeds as described above while the height of the tip-holder assembly adjusts dynamically according to the above feed-back mechanism.

In fig. 1 we show particle trajectories, viewed from the side along the (101) direction and from the top (along the (111) direction, d and h) for constant tip-height simulations and a static tip (i.e., hard but reactive tip), at two tip heights, h_1 and h_3. Trajectories for a complete scan at the low tip height $h_3(1)$, are shown in a and d (the scan direction is from left to right). The horizontal lines are the static tip-particle trajectories (only 3 tip particles out of the 4 are visible from this viewing direction). In figs. 1b and 1c particle trajectories are shown at the beginning and towards the end of the scan. As seen in fig. 1b the interaction with the tip triggers local displacements of substrate particles. In particular, the atom in the top layer right below the tip *drops* to an *interstitial position* in the second layer. This is seen clearly in fig. 1c, where the interstitial atom is marked by an arrow. Note that once the tip advances, the localized defect induced by the tip anneals (compare the left part of the scan in figs. 1b and 1c). In comparison, locating the tip at $h_1(1)$, in the region of attractive interaction, results in a *localized outward displacement* of atoms in the substrate top layer (see figs. 1i and 1j, where the displaced particle is marked by an arrow). The dependence on the scan geometry which affects the relative tip to substrate atoms bond distances, orientations and coordination and subsequently the resultant forces, is demonstrated by comparing the trajectories shown in figs. 1a–1d and 1e–1h. As seen, the between-row scan, $h_3(2)$, produces a more significant damage to the surface due to the bonding geometry generating top layer vacancies (2 atoms attached to the tip, figs. 1e and 1g).

Records of the forces on the tip atoms for the three scan heights versus tip location and versus time are shown in figs. 2a–2f and 2g and 2h, respectively. We start with the time-histories of the $h_1(1)$ and $h_3(1)$ scans (figs. 2g and 2h). For the high-tip scan, $h_1(1)$ (fig. 2g) the tip experiences throughout an attractive force ($F_z < 0$) towards the substrate, increasing as the tip advances laterally in the regions between substrate atoms. A different situation is encountered in the low-tip scan, $h_3(1)$ (fig. 2h). Here, as the tip is lowered it initially attracts to the surface, followed by a decrease in the force as the tip enters the repulsive region, and subsequently experiencing a repulsive interaction ($F_z > 0$ at ~ 30 tu). This is then followed by a sharp attraction (~ 40 tu), culminating in a resultant *attractive force* ($F_z \approx -1\ \epsilon/\sigma$), although the tip at this point is in intimate contact with the surface, which would have been expected to yield a strong repulsion. The dynamical mechanism underlying the observed attraction is the generation of surface interstitial defects (see also figs. 1a–1d). Thus, the interaction with the tip can induce *local* rearrangement in the substrate and consequently can alter (even reverse the sign) of the resultant recorded forces. Further lateral scanning over substrate atoms is

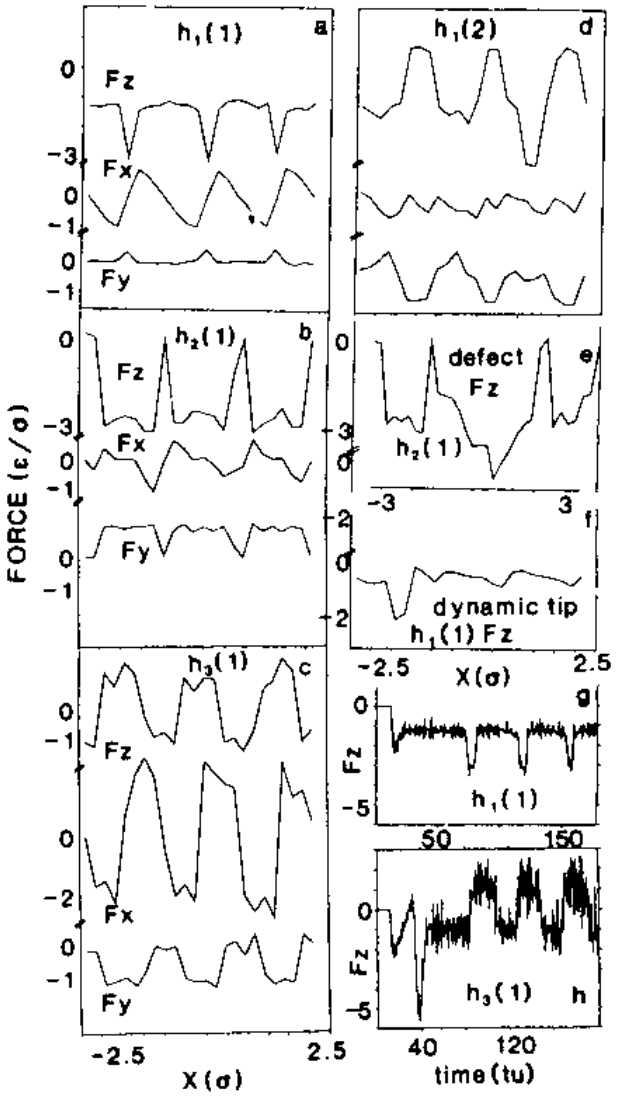

Fig. 2. (a–c) Forces on the tip atoms for the high, intermediate and low tip scans along the X $(1\bar{1}0)$ direction for scan 1. (d) Forces on the tip for the between-the-rows scan (2); the F_z force on the tip in a $h_2(1)$ scan for a defective surface is shown in (e) and in an $h_1(1)$ scan for a dynamic tip (f); (g, h) F_z force on the tip in high, $h_1(1)$, and low, $h_3(1)$, scans versus time, respectively. These time records include the stage of lowering the tip. All others start after equilibration at the indicated height. Distance in units of σ, time in units of tu and force in units of $\epsilon/\sigma = 1.6572 \times 10^{-9}$ N.

characterized by periodic oscillations in the force which reflect the substrate periodicity.

The dependence of the character of the recorded forces versus position on tip height is illustrated in figs. 2a–2c for scan 1. These records were obtained after the initial equilibration, with the tip lowered to the desired height. Significant variations in the magnitudes and character of the forces are observed depending upon the tip separation from the surface. For example, the F_z component at $h_1(1)$ is overall attractive with sharp negative spikes which for the intermediate tip height, $h_2(1)$, turn into broad attractive plateaus when the tip is scanning between surface atoms. For the low-tip configuration, fig. 2c, passage between surface atoms is exhibited by broad repulsive peaks. Spatial variations of the potential energy surface are exhibited

by comparison of the two scans at the h_1 height (figs. 2a and 2d). Note in particular the changes in F_z, and the change in magnitudes of F_x and F_y. These characteristics portraying the surface structure and the spatial variation of the potential are within the current estimates of resolution in AFM [2].

A comparison between the F_z records for an ideal surface (fig. 2b) and for a defective surface (fig. 2e) reveals the scale and character of variations caused by microscopic modifications in the surface morphology. Here, the surface was initially equilibrated with a top layer vacancy at the location of the fourth atom from the right in the row directly under the lower-most tip atom (see fig. 1d). Examination reveals that in course of the scan the tip caused major rearrangement of the defective region via a complicated sequence of atomic displacements involving first and second layer atoms.

Simulations were also performed, at constant-height, for tip atoms which were allowed to evolve dynamically. The recorded F_z force for a high-tip scan, $h_1(1)$, shown in fig. 2f, exhibits a decrease in magnitude originating from a relaxation of the tip, occurring mainly at the beginning of the scan, and shifts and pronounced asymmetry of characteristic features (compare to F_z in fig. 2a), connected with a stick–slip behavior exhibited by the lower-most tip atom as the scan progresses (see below).

We turn next to *constant-force simulations* employing an initially ordered tip consisting of 102 atoms (exposing a 16 atom (111) facet) scanning a 6 layer substrate with 100 atoms/layer. In these simulations both the substrate and tip atoms respond dynamically and the scan rate is half of that described above. In fig. 3 we show results for a scan, for a constant force value $F_{z,\mathrm{ext}} = -13.0$ (i.e., 2.15×10^{-8} N). Side views of the system trajectories at the beginning and end stages of the scan are shown in figs. 3a, 3b and 3c, respectively. As seen the tip–substrate interaction induces local modifications of the substrate and tip structure, which are transient and similar to those observed in the constant-height simulations. The recorded force on the tip-holder in the X^* direction is shown in fig. 3d. While the normal force, F_z, fluctuates around the prescribed value as required, the force along the scan direction (F_x, in fig. 3d) exhibits a periodic modulation portraying the periodicity of the substrate. Most significant is the stick–slip behavior signified by the asymmetry in F_x (observed also in the real-space atomic trajectories in figs. 3a and 3b). Here, the tip atoms closest to the substrate attempt to remain in a favorable bonding environment as the tip-holder assembly proceeds to scan. When the forces on these atoms due to the other tip atoms exceed the forces from the substrate, they move rapidly to minimize the F_x force, by breaking their current bonds to the surface and forming new bonds in a region translated by one unit cell along the scan direction. We note that our constant-force simulation method corresponds to the experiments in ref. [6] in the limit of a stiff wire (lever) and thus the stick–slip phenomena which we observed are a direct consequence of the interplay between the surface forces

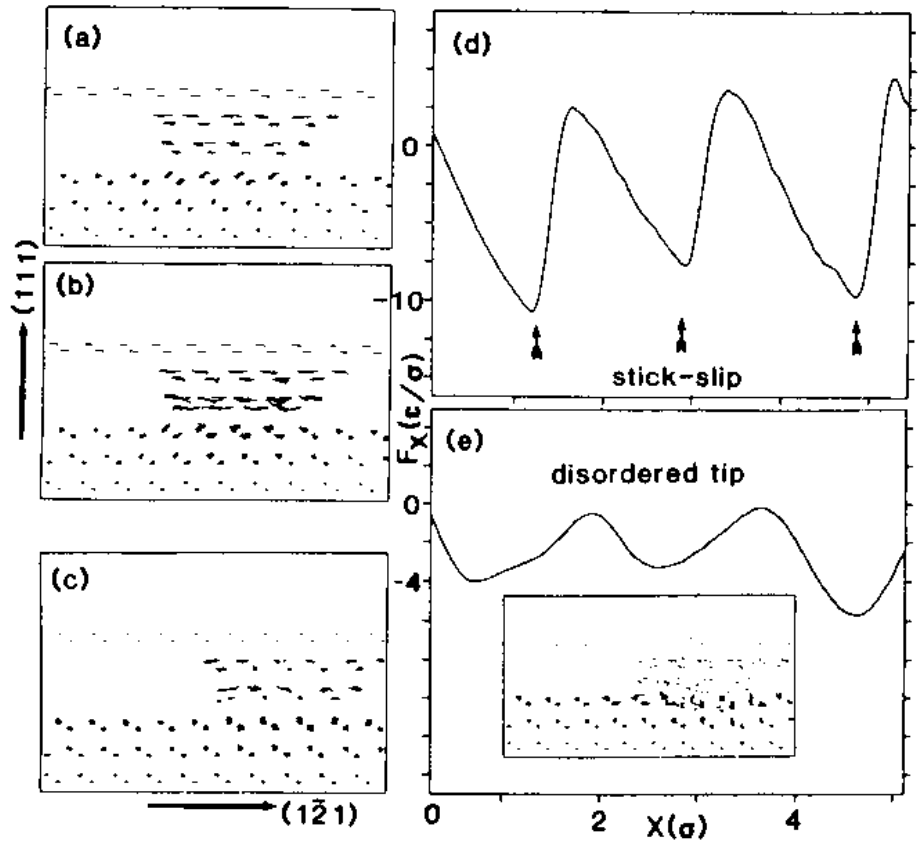

Fig. 3. (a–c) Particle trajectories in a constant-force simulation viewed along the $(10\bar{1})$ direction just before (a) and after (b) a stick–slip event and towards the end of the scan (c), for a large, initially ordered, dynamic tip. (d) The recorded F_x, exhibiting stick–slip behavior. (e) The F_x force in a constant-force scan ($F_{z,\mathrm{ext}} = 1.0$) employing a glassy static tip, exhibiting the periodicity of the substrate. Shown in the inset are the real-space trajectories towards the end of the scan, demonstrating the tip-induced substrate local modifications.

and interatomic interactions in the tip. The F_x force which we record corresponds to the frictional force. From the extrema in F_x (fig. 3d) and the load ($F_{z,\mathrm{ext}}$) used we obtain a coefficient of friction $\mu = |F_x|/|F_{z,\mathrm{ext}}| = 0.77$, in the range of typical values obtained from tribological measurements in vacuum.

Finally, we show in fig. 3e the frictional force obtained in simulations employing a disordered static 102-atom tip, prepared by quenching of a molten droplet, scanning under a load $F_{z,\mathrm{ext}} = 1.0$. The significance of this result lies in the periodic variation of the force reflecting the atomic structure of the substrate. This demonstrates that microscopic investigations of structural characteristics and tribological properties of crystalline substrates are not limited to ordered tips [6].

References

[1] G. Binnig, H. Rohrer, Ch. Gerber and E. Weibel, Phys. Rev. Letters 50 (1983) 120; G. Binnig and H. Rohrer, IBM J. Res. Develop. 30 (1986) 355.
[2] G. Binnig, C.F. Quate and Ch. Gerber, Phys. Rev. Letters 56 (1986) 930.
[3] J.N. Israelachvili, Acc. Chem. Res. 20 (1987) 415.

[4] J.N. Israelachvili, P.M. McGuiggan and A.M. Homola, Science 240 (1988) 189.
[5] P.K. Hansma and J. Tersoff, J. Appl. Phys. 61 (1986) R1;
R.J. Colton and J.S. Murday, ONR Rev., in press.
[6] C.M. Mate, G.M. McClelland, R. Erlandsson and S. Chiang, Phys. Rev. Letters 59 (1987) 1942.
[7] J.M. Soler, A.M. Baro, N. Garcia and H. Rohrer, Phys. Rev. Letters 57 (1986) 444;
see comment by J.B. Pethica, Phys. Rev. Letters 57 (1986) 3235.
[8] J.K. Gimzewski and R. Moller, Phys. Rev. B 36 (1987) 1284.
[9] F.H. Stillinger and T.A. Weber, Phys. Rev. B 31 (1985) 5262.
[10] U. Landman, W.D. Luedtke, R.N. Barnett, C.L. Cleveland, M.W. Ribarsky, E. Arnold, S. Ramesh, H. Baumgart, A. Martinez and B. Khan, Phys. Rev. Letters 56 (1986) 155;
F.F. Abraham and J.Q. Broughton, Phys. Rev. Letters 59 (1987) 64;
W.D. Luedtke and U. Landman, Phys. Rev. B 37 (1988) 4656;
U. Landman, W.D. Luedtke, M.W. Ribarsky, R.N. Barnett and C.L. Cleveland, Phys. Rev. B 37 (1988) 4637, 4647;
F.F. Abraham and I.P. Batra, Surface Sci. 163 (1985) L752.
[11] F.F. Abraham, I.P. Batra and S. Ciraci, Phys. Rev. Letters 60 (1988) 1314.
[12] See U. Landman and W.D. Luedtke, in: Atomistic Modeling in Materials: Beyond Pair-Potentials, Ed. V. Vitek (Plenum, New York, 1988).
[13] See U. Landman, in: Computer Simulation Studies in Condensed Matter Physics: Recent Developments, Eds. D.P. Landau, K.K. Mon and H.-B. Schuttler (Springer, Berlin, 1988).
[14] See U. Landman, D.W. Luedtke and M.W. Ribarsky, in: New Materials Approaches to Tribology: Theory and Applications, Eds. L.E. Pope, L. Fehrenbacher and W.O. Winer (MRS, Boston, 1989).